

1  
2  
3 **Application of field-portable-XRF for the determination**  
4 **of trace elements in deciduous leaves from a mine-**  
5 **impacted region**  
6  
7

8 **Andrew Turner<sup>\*1</sup>, Chor Chi Chan<sup>1</sup>, Murray T. Brown<sup>2</sup>**

9  
10 *<sup>1</sup>School of Geography, Earth and Environmental Sciences and <sup>2</sup>School of Biological and*  
11 *Marine Sciences, Plymouth University, Drake Circus, Plymouth PL4 8AA, UK*  
12  
13  
14

15 \*Corresponding author: e-mail: aturner@plymouth.ac.uk  
16  
17

18 Accepted in Chemosphere 21 June 2018

19 <https://doi.org/10.1016/j.chemosphere.2018.06.110>

20 Embargoed until 21 June 2019  
21

22 **Abstract**

23 Deciduous leaves ( $n = 87$ ) from beech (*Fagus sylvatica*), birch (*Betula* spp.) and oak  
24 (*Quercus* spp.) trees have been collected from three metal mine-impacted sites in southwest  
25 England and tested for concentrations of trace elements (As, Cu, Pb and Zn) using a field-  
26 portable-x-ray fluorescence (FP-XRF) spectrometer configured in a low density mode and  
27 housed in a stand. When intact leaves were analysed directly, mean detection limits ranged  
28 from about 10 (As) to 70  $\mu\text{g g}^{-1}$  (Cu) on a fresh weight basis; after freeze-drying, respective  
29 limits increased to about 20 and 120  $\mu\text{g g}^{-1}$  on a dry weight basis. Within these constraints,  
30 As and Zn were detected in samples from all genera, with concentration differences between  
31 fresh and dry states attributed to the mass of water present and its propensity to attenuate x-  
32 rays. A comparison with As and Zn concentrations in local soils and determined by XRF in a  
33 higher density mode revealed different accumulation and exclusion characteristics among the  
34 three genera of tree. In contrast, and despite soil concentrations that were similar to those of  
35 Zn, Cu was detected in only two dried leaves and Pb evaded detection throughout. Pooled  
36 results from the study showed good agreement with independent results derived from ICP  
37 following acid digestion, with a slope that was close to unit value. Accordingly, the XRF  
38 approach is able to provide a rapid assessment of the levels of certain trace elements in  
39 leaves from contaminated sites, with the configuration deployed on site having potential to  
40 deliver immediate results.

41

42 **Keywords:** deciduous leaves; field-portable-XRF; arsenic; zinc; soils; biomonitoring

43 **1. Introduction**

44 Although mosses and epiphytic lichens have gained widespread use in biomonitoring of  
45 airborne trace element pollution, their absence in some urban and industrialised areas has  
46 resulted in the study of higher plants (Bargagli et al., 2003; Aničić et al., 2011; Serbula et al.,  
47 2014). Many tree species are tolerant of high environmental concentrations of trace elements  
48 and leaves are often the main sink for pollutants (Bargagli, 1998). Thus, as well as providing  
49 a means of increasing the trace element content of top soils through leaf deposition-  
50 decomposition and increasing trace element exposure to consuming organisms, leaves act as  
51 potential indicators of both contaminated soil, through uptake via the root system, and  
52 polluted air, through wet and dry deposition (Franiel and Babczyńska, 2011; Dimitrijević et  
53 al., 2016; Pająk et al., 2017).

54

55 At sites impacted by contemporary or historical metalliferous mining, and where the  
56 presence of elevated environmental concentrations of many trace elements is a concern,  
57 deciduous and evergreen tree leaves have been commonly employed as indicators of soil  
58 contamination (Unterbrunner et al., 2007; Dmuchowski et al., 2014; Nirola et al., 2015;  
59 Stefanowicz et al., 2016). Here, capture and uptake of a trace element is from a large soil  
60 volume, with the concentration of an element in the leaves reflecting the availability of the  
61 element in the soil rather than its total concentration. Strictly, and to act as a true  
62 bioindicator, uptake through the roots should be relatively constant over a wide gradient of  
63 trace element concentrations in the soil such that there should be a linear relationship  
64 between concentrations in the leaves and in the soil (Baker et al., 2000; Kabata-Pendias and  
65 Pendias, 2001). However, some trees may act as excluders for certain elements by inhibiting  
66 their uptake into roots, even at high external concentrations in the soil, while others may act  
67 as hyper-accumulators which are able to tolerate high concentrations in their leaves, even at  
68 low external concentrations (Madejón et al., 2004; Schmidt et al., 2016); the latter are,

69 therefore, particularly attractive as phytoremediators of highly contaminated soils  
70 (Antosiewicz et al., 2008; Dimitrijević et al., 2016).

71

72 With different possible sources of trace elements (from the atmosphere and soil) and  
73 potentially confounding issues of hyper-accumulation and exclusion, the analysis of a large  
74 number of leaf samples is often required at contaminated sites, with repeat visits sometimes  
75 necessary. Conventional analysis of leaves involves digestion of the matrix in concentrated  
76 mineral acid followed by trace element determination by, for example, inductively coupled  
77 plasma spectrometry or atomic absorption spectrometry, but this approach can be time- and  
78 resource-consuming and generate large quantities of hazardous waste. As an alternative,  
79 plant material may be determined non-destructively by x-ray fluorescence (XRF)  
80 spectrometry. Here, samples are typically dried, milled and packed before being excited by  
81 an x-ray beam, with the expulsion of inner electrons of an atom accompanied by electrons  
82 cascading from higher orbitals and the emission of characteristic fluorescent x-rays  
83 (Sacristán et al., 2016; Towett et al., 2016).

84

85 In order to further minimise sample preparation, it may be assumed that the plant matrix has  
86 similar characteristics to thin plastic films in terms of the absorption, scattering and  
87 fluorescence of x-rays, and analyse material intact (i.e. without milling or packing) using an  
88 XRF algorithm that is calibrated for low density matter. This approach was recently tested  
89 and validated both in the laboratory and in the field on coastal and marine macroalgae (Bull  
90 et al., 2017; Turner et al., 2017) and is trialled in the present study on deciduous leaves.  
91 Specifically, the current investigation focuses on the trace metalloid, As, and the trace metals  
92 Cu, Pb and Zn, in both common leaves and in soils (with the latter employing more  
93 established XRF protocols) at three sites impacted by historical, non-ferrous mine waste.

94 Although tests were performed solely in the laboratory, the potential for applying the  
95 approach in the field is also addressed.

96

## 97 **2. Materials and methods**

### 98 *2.1. Sampling*

99 Sampling of leaves and soils was undertaken at three sites impacted by historical (19<sup>th</sup>  
100 century), non-ferrous metal mining activities in west Devon, south west England. The  
101 geology of the region is dominated by fine-grained sedimentary sequences and chert but with  
102 outcrops of granite and slates, and soils are mainly brown earths that are well-drained but  
103 subject to slight seasonal waterlogging (Rawlins et al., 2003). The region is sparsely  
104 populated, with occasional small settlements and farms, and current land use is dominated by  
105 agriculture and managed woodland. The first site (S1) was on Dartmoor National Park in the  
106 vicinity of a series of relatively small, disused copper mines (digital co-ordinates: 50.5130, -  
107 4.1116; 85 m asl). The second and third sites were within the UNESCO district of the Tamar  
108 Valley at locations influenced by more extensive mining and processing facilities for both  
109 copper and arsenic; specifically, S2 was adjacent to an old but functional adit (50.5361, -  
110 4.2081; 50 m asl) and S3 was along the northern edge of a large spoil tip (50.5385, -4.2214;  
111 78 m asl).

112

113 Each site was visited during mid-autumn (early November) in 2016, following a period of  
114 dry weather and as deciduous foliage was being shed. A total of 87 leaves were collected by  
115 hand and using plastic tweezers from trees that were common to all sites and that usually  
116 occurred in clusters but were occasionally solitary: namely, beech (*Fagus sylvatica*), birch  
117 (*Betula* spp., including *B. pendula*) and oak (*Quercus* spp.). Specifically, three leaves were  
118 taken from lateral branches at a height of about 2 m from between one and five trees of each  
119 genus (depending on their abundance and accessibility) and stored in individual zip-lock

120 specimen bags in a dark polyethylene box. Soil samples, of about 300 g and to depths of  
121 around 10 cm, were collected from under the canopies of three trees from each location  
122 using a plastic trowel and were stored likewise.

123

## 124 *2.2. Leaf sample processing and XRF analysis*

125 On return to the laboratory, leaf surfaces were wiped gently with three-ply blue roll to  
126 remove any visibly adherent material and weighed on a five-figure Sartorius balance. Fresh  
127 samples were then analysed for a suite of elements, of which As, Cu, Pb and Zn as important  
128 contaminants of non-ferrous mining are the focus of the present study, by energy dispersive,  
129 field-portable (FP-)XRF using a battery-powered Niton XRF analyser (model XL3t 950 He  
130 GOLDD+) which was configured, nose-upwards, in a bench-top accessory stand and  
131 activated remotely by a laptop connected via USB. In order to minimise any artefacts arising  
132 from variations in geometry or thickness, an area of the upper blade midway between the  
133 mid-rib and margin, and free from any sign of infection, was selected for analysis. This area  
134 was measured for thickness using Allendale digital callipers before being positioned directly  
135 above the XRF detection window, a process aided by imagery from an integrated CCD  
136 camera and, where necessary, polyethylene blocks outside of the x-ray beam acting as  
137 weights. Once the shield of the stand was closed, measurements, with appropriate thickness  
138 correction and in a low-density plastics mode, were undertaken for equal counting periods in  
139 a main energy range (50 kV/40  $\mu$ A) and low energy range (20 kV/100  $\mu$ A). Counting was  
140 trialled up to ten minutes but a total period of 120 seconds was selected as a suitable  
141 timescale that appeared to provide sufficiently low counting errors yet maximise the number  
142 of elements detected. Spectra arising from both energy ranges were quantified by  
143 fundamental parameters to yield elemental concentrations in  $\mu\text{g g}^{-1}$  and a counting error of  
144  $2\sigma$  (95% confidence) that were downloaded to the laptop using Niton Data Transfer  
145 software.

146  
147  
148  
149  
150  
151  
152  
153  
154  
155  
156  
157  
158  
159  
160  
161  
162  
163  
164  
165  
166  
167  
168  
169

In order to correct for the mass contribution of water and to evaluate the effects of the aqueous phase on x-ray absorption, leaves were frozen, dried for 24 h in an Edwards Super Modulyo freeze-drier and reweighed before being re-analysed at the approximate positions measured while fresh. With no suitable biological reference films available, performance and precision were evaluated by analysing a Niton plastic reference disc (PN 180-619, LOT#T-18) certified for a suite of elements (including As and Pb) at regular intervals during each measurement session.

### *2.3. Soil sample processing, characterisation and XRF analysis*

Soil samples were freeze-dried for 48 h before being ground with a ceramic pestle and mortar and sieved through a 63  $\mu\text{m}$  stainless steel sieve. A sufficient quantity of each fractionated sample was then used to completely fill a series of Chemplex series 1400 XRF sample cups (21-mm internal diameter) that were collar-sealed with 3.6  $\mu\text{m}$  SpectraCertified Mylar polyester film. For XRF analysis, cups were placed centrally over the detector window with the collar-sealed Mylar surface face-down, and measurements were conducted for 60 seconds in a higher density mining mode, comprising successive counting periods of 20 s each in a main (50 kV/40  $\mu\text{A}$ ), low (20 kV/100  $\mu\text{A}$ ) and high (50 kV/40  $\mu\text{A}$ ) energy range. Spectra were quantified and concentrations downloaded to the laptop as above. For quality assurance purposes, sufficient quantities of a Sigma-Aldrich RTC loam certified for As and Zn (MSL-MSL101) and a National Institute of Standards and Technology soil certified for a broader suite of elements (SRM 2709a) were packed into XRF cups and analysed likewise.

170 Ten g portions of the remaining fractionated soil samples were equilibrated with 25 ml  
171 aliquots of deionised water in a series of 50 ml polypropylene centrifuge tubes and the pH  
172 measured using a Meterlab PHM210 pH meter and Hach pHC2051-8 electrode.

173

#### 174 *2.4. Leaf digestion and analysis by ICP*

175 As an independent and more sensitive measure of the metal and metalloid content of leaves,  
176 dried and infection-free whole leaf samples ( $n = 28$ ) from different trees and sites and, in  
177 triplicate, a powdered leaf reference material (GBW 08501, peach leaves) were acid-digested  
178 and analysed by inductively coupled plasma-mass spectrometry (ICP-MS). Thus, samples  
179 were accurately weighed into individual Teflon tubes to which 6 ml aliquots of HNO<sub>3</sub>  
180 (Fisher Chemical TraceMetal™ Grade) were added. The contents were digested in a CCEM  
181 MARS 5 XPRESS microwave at 1600 W for 45 min before being allowed to cool. Digests  
182 were then washed into individual 25 ml volumetric flasks and diluted to mark with Millipore  
183 Milli-Q water.

184

185 Digests were analysed for As, Cu, Pb and Zn using a collision cell-ICP-MS (Thermo X-  
186 series II, Thermoelemental, Winsford, UK) with a concentric glass nebuliser and conical  
187 spray chamber. RF power was set at 1400 W and coolant, auxiliary, nebuliser and collision  
188 cell gas flows rates were 13 L Ar min<sup>-1</sup>, 0.70 L Ar min<sup>-1</sup>, 0.786 L Ar min<sup>-1</sup> and 3.5 mL 7%  
189 H<sub>2</sub> in He min<sup>-1</sup>, respectively. The instrument was calibrated externally using four standards  
190 prepared by dilutions of a QC 26 multi-element solution (CPI International, Amsterdam) in  
191 0.1 M HNO<sub>3</sub>, and internally by the addition of 100 µg L<sup>-1</sup> of In and Ir to all samples and  
192 standards. Data were acquired over a dwell period of 10 ms, with 50 sweeps per reading and  
193 three replicates and were converted to dry weight concentrations (in µg g<sup>-1</sup> dw) from the  
194 volume of diluted digest and mass of leaf digested. Limits of detection on this basis were <  
195 0.5 µg g<sup>-1</sup> for all elements analysed.



196

## 197 2.5. Quality assurance

198 Dry weight concentrations arising from XRF or ICP analyses of the various reference  
199 materials (plastic disc, soils and leaves) are compared with certified or indicative values in  
200 Table 1. Thus, within the levels of uncertainty and error, agreement was accomplished by  
201 XRF for As and Pb in polyethylene and As and Zn in NIST soil and by ICP for As, Pb and  
202 Zn in peach leaves, with mean measured concentrations in the remaining cases within 25%  
203 of the respective mean certified values. Precision, as one standard deviation relative to the  
204 mean, was < 5% in all cases with the exception of Zn in peach leaves (15%) and As, Cu and  
205 Pb in NIST soil (between 13 and 24%).

206

207

## 208 3. Results and Discussion

### 209 3.1. Leaf and soil characteristics

210 Table 2 shows the number of leaves taken from each genus of tree at each site, where  
211 multiples of three reflect the number of trees sampled. Overall, 87 samples were collected  
212 for analysis with a roughly equal distribution among genera but differences between sites  
213 that reflected tree abundance and accessibility. At S1, average leaf size, based on fresh  
214 weight, decreased in the following order: *Quercus* > *Fagus* > *Betula*; at S2 and S3, tree  
215 growth appeared to be more stunted and the size of oak and beech leaves were reduced  
216 considerably such that average leaf size across the three genera was similar. The percentage  
217 contribution of water to leaf mass averaged 42% for *Fagus* and *Betula* and 21% for *Quercus*,  
218 with leaves in the latter genus being distinctly drier at S2 and S3. Leaf thickness through the  
219 measurement area was not significantly different ( $p > 0.05$  according to a series of paired or  
220 two-sample *t*-tests performed in Minitab v17) between genus, sampling site, or fresh and dry

221 state, with overall averages of 0.26 mm, 0.27 mm and 0.34 mm for *Betula*, *Fagus* and  
222 *Quercus*, respectively.

223

224 The pH of the soil samples, together with trace element content determined by XRF in a  
225 conventional and established soils mode (Kalnicky and Singhvi, 2001; Radu and Diamond,  
226 2009), are summarised in Table 3. Thus, average pH ranged from about 4.9 to 5.5, with  
227 individual measurements ranging from about 3.9 at S2 to 6.3 at S1. Average concentrations  
228 of Pb and Zn were similar among the three sites, with individual concentrations ranging from  
229 about 70 to 300  $\mu\text{g g}^{-1}$  dw and 90 to 290  $\mu\text{g g}^{-1}$  dw, respectively. In contrast, and consistent  
230 with the relative significance of historical mining for Cu and As and legacy contamination,  
231 mean concentrations of Cu were three- to four-fold higher and mean concentrations of As  
232 about 50 and 130 times higher at S2 and S3 than corresponding mean concentrations at S1.

233

### 234 3.2. XRF detection limits in leaves

235 For a specific counting time and mode of application, the Niton FP-XRF provides  
236 measurement limits of detection (LODs) for each element that are dependent on the  
237 characteristics of the sample, including its density, thickness and chemical composition, and  
238 that are calculated from three counting errors arising from the analysis (or  $2\sigma \times 1.5$ ;  
239 99.7% confidence interval). LODs for As, Cu, Pb and Zn for all samples analysed in the  
240 present study are summarised in Table 4, with concentrations given on a fresh weight (fw) or  
241 dry weight (dw) basis depending on the nature of sample processing. Thus, for a given  
242 element, LODs span about an order of magnitude, with values generally related to the  
243 reciprocal of sample thickness, but that were not significantly different ( $p > 0.05$  according  
244 to one-way ANOVA performed in Minitab v17) between the different genera of tree. For all  
245 elements, average LODs were at least 50% greater for leaves analysed freeze-dried than  
246 when fresh. With thicknesses that were statistically indistinguishable between the dry and

247 fresh states and the propensity of water to absorb low energy x-rays, this observation is,  
248 perhaps, counterintuitive. However, based on similar observations made during the XRF  
249 analysis of fresh and dried macroalgae (Turner et al., 2017), we attribute the discrepancy to a  
250 greater flexibility of biological material when fresh, allowing blades to be positioned closer  
251 to the detector window of the instrument. This effect also resulted in precisions, derived  
252 from repeat measurements of the same leaf area, that were better when samples were  
253 analysed in the fresh state (between 10 and 20%) than when analysed after freeze-drying  
254 (between 15 and 25%).

255

### 256 *3.3. Elemental concentrations in leaves*

257 Table 5 gives the number of cases that As, Cu, Pb and Zn were detected in the leaf samples  
258 along with summary statistics for the resulting concentrations. Using FP-XRF, As was  
259 detected in 13 samples when analysed dry with concentrations ranging from about 13 to 360  
260  $\mu\text{g g}^{-1}$  dw, and detection was limited to samples taken adjacent to the spoil heap (S3) and  
261 was dominated by oak leaves ( $n = 8$ ). The metalloid was detected in 19 samples when  
262 analysed fresh, with concentrations ranging from about 5 to 450  $\mu\text{g g}^{-1}$  fw and, after  
263 correction for the amount of water present, from about 12 to 500  $\mu\text{g g}^{-1}$  dw. Detection  
264 exhibited a similar site and genus distribution to the dried samples but a number of positives  
265 were returned for samples of birch taken at S1.

266

267 Zinc was detected in 47 samples analysed dry with concentrations ranging from about 30 to  
268 660  $\mu\text{g g}^{-1}$  dw, and both detection and the highest concentrations were most frequent among  
269 birch leaves from S1 and S3. When analysed fresh, Zn was detected in 40 samples and at  
270 concentrations ranging from about 20 to 280  $\mu\text{g g}^{-1}$  fw and, after correction for water  
271 content, from about 30 to 440  $\mu\text{g g}^{-1}$  dw, with a similar site and genus distribution to that  
272 derived from analysis of the dried samples. Copper was detected by XRF in just two dried

273 oak leaves from S3, despite lower measurement detection limits for the metal in fresh leaves  
274 (Table 4), and Pb was never detected by the instrument.

275

276 Also shown in Table 5 are concentrations of As, Cu, Pb and Zn returned by ICP following  
277 acid digestion of a selection of whole, freeze-dried leaves ( $n = 28$ ) that encompassed each  
278 genera from all three sites. Here, each element was detected in all samples tested, with  
279 results spanning greater concentration ranges than the corresponding results returned by  
280 XRF.

281

### 282 *3.4. Comparison of concentrations derived from fresh and dry analyses of leaves*

283 In order to evaluate the impacts of internal water on the results, hence the feasibility of  
284 measuring elements in fresh leaves by XRF on site, concentrations returned directly for  
285 freeze-dried leaves are compared with dry weight concentrations derived indirectly from the  
286 analysis of fresh samples and after correction for water content in Figure 1 (note that the  
287 comparison is restricted to cases where detection was accomplished by both approaches on  
288 the same sample;  $n = 11$  for As and  $n = 32$  for Zn). Thus, despite different geometries and  
289 distances from the detector window incurred by the two states, potential differences in the  
290 precise location of sample analysed on successive occasions and the heterogeneous  
291 distribution of water within leaves, both data sets exhibited a high degree of association  
292 when subject to Pearson's moment correlation analysis performed using the data analysis  
293 ToolPak in Excel 2016 ( $r > 0.85$ ,  $p < 0.001$ ). Linear regression analysis performed in Excel  
294 2016 also revealed equations of best fit with either a y-intercept or that were forced through  
295 the origin that were highly significant ( $p < 0.001$ ), but regression slopes indicated  
296 concentrations that were not equivalent. Specifically, the gradient defining the fresh to dry  
297 converted concentrations versus dry concentrations determined directly were either above  
298 (As) or below (Zn) unit value.

299

300 In addition to its contribution to leaf mass and its alteration of sample geometry, water may  
301 influence dry weight concentrations derived from fresh analyses through the absorption of  
302 primary and secondary x-rays, an effect whose potential significance can be evaluated  
303 theoretically. Thus, the mass attenuation coefficient for water at 10 keV, or the approximate  
304 energies of the main K-level emission lines for both As and Zn, is  $5.3 \text{ cm}^2 \text{ g}^{-1}$  (Hubbell and  
305 Seltzer, 1996). This yields a half-value layer (where 50% of incident radiation is attenuated)  
306 of about 1.3 mm, and attenuation of 10% for a layer of about 0.4 mm, or the upper thickness  
307 of the leaves tested. Most leaves that were Zn-positive when analysed both fresh and dry  
308 (and as plotted in Figure 1) were from *Betula* spp., whose internal water content was about  
309 60%, while those that were As-positive when analysed in both states were from *Quercus*  
310 spp., whose water content was about 20%. On this basis, therefore, we would predict the  
311 analysis of fresh samples of consistent thickness to affect the results for Zn to a greater  
312 extent than those of As, largely through the absorption of both irradiating and fluorescent x-  
313 rays by samples of a higher water content. This assertion is qualitatively consistent with the  
314 data in Figure 1 in that the regression slopes for Zn are smaller than those for As, but does  
315 not explain why the slope for As lies above unit value. A confounding issue in this respect is  
316 the presentation of a flatter and more uniform surface that is closer to the detector when  
317 samples are fresh and more pliable, and as described above.

318

### 319 *3.5. Comparison of concentrations derived by XRF and ICP analyses of leaves*

320 A comparison of the results obtained by ICP, following digestion in concentrated  $\text{HNO}_3$ ,  
321 with those returned by the FP-XRF revealed no false negatives or false positives; that is, lack  
322 of detection by the XRF was not accompanied by a measurement by ICP that exceeded the  
323 corresponding LOD of the Niton XL3t and concentrations returned by the XRF were never  
324 accompanied by ICP measurements that were below detection limit of the mass

325 spectrometer. Where concentrations were returned by both ICP and XRF (either on fresh  
326 leaves or freeze-dried samples), results are plotted in Figure 2, with As and Zn data shown  
327 individually and, with Cu, in combination. Despite the potential limitations and sources of  
328 error of XRF outlined above and fundamental discrepancies in the leaf part examined (XRF  
329 probes a small area of blade while ICP necessitates digestion of the whole sample), both  
330 correlation and linear regression analyses performed in Excel 2016 revealed a significant  
331 relationship between the results from both analytical approaches in all cases ( $p < 0.001$ ).  
332 Agreement between XRF and ICP, defined as the deviation of the gradient of the regression  
333 equation (forced through the origin) from unit slope, was within 30% for both As and Zn and  
334 within 10% when data for all trace elements were pooled. In all cases, however, closer  
335 agreement resulted when leaves were analysed fresh than when dry, an effect that may be  
336 related to the ability to manoeuvre samples closer to the detector window when in the fresh  
337 state than after freeze-drying (see above).

338

### 339 *3.6. Potential application of FP-XRF for biomonitoring*

340 The present study has explored the feasibility of measuring trace elements in common  
341 deciduous leaves directly and non-destructively by FP-XRF. The approach is capable of  
342 determining many key elements to dry weight concentrations of a few tens of  $\mu\text{g g}^{-1}$  and is  
343 particularly suited to environments where there are clear and significant sources of  
344 contaminants. Of the metals and metalloids considered herein, As, a toxic metalloid, and Zn,  
345 a micronutrient, were most readily detected in a variety of leaf samples from three sites,  
346 and agreement with concentrations derived independently from ICP following acid digestion  
347 was sufficiently strong and significant to at least partly satisfy the EPA definitive level data  
348 criterion (Environmental Protection Agency, 2007). Being capable of measuring elements in  
349 fresh samples, with conversion of concentrations to a dry weight basis accomplished to a  
350 good approximation by correction for internal water content, the method has the potential for

351 monitoring in the field. Here, the instrument would be configured in a portable test stand as  
352 described elsewhere (Turner et al., 2017) and activated remotely using a laptop under the  
353 operating conditions outlined above. With the simultaneous capability of measuring trace  
354 metals and metalloids in soils, the approach can deliver a rapid assessment of site  
355 contamination, element compartmentalisation and uptake-exclusion-accumulation.

356

357 Although the principal objectives of the study were to explore the potential application of  
358 FP-XRF to the biomonitoring of leaves, the results have demonstrated differences in element  
359 accumulation among the three genera of tree that were most significant at S3 and as  
360 illustrated by the direct measurements of dried samples in Figure 3. Thus, here, As was  
361 highly enriched in local soils (Table 3) because of the historical mining for the metalloid but  
362 concentrations were two or three orders of magnitude lower in the leaves analysed;  
363 specifically, As was detected in two samples of *Fagus* and *Betula* spp. but was detected in all  
364 samples of *Quercus* spp. It would appear, therefore, that at least the first two genera are  
365 excluders of As in that, despite extremely high concentrations in local soils, there is active  
366 inhibition by the root system. In contrast, Zn at S3 exhibited no elevated contamination in  
367 soil relative to concentrations at S2 and S3 (Table 3) and, unlike As, showed no measurable  
368 accumulation by *Quercus* spp. leaves. However, the metal was detected in every sample of  
369 *Betula* and at concentrations that always exceeded the mean concentration of Zn in local soil  
370 and that are considered to exert toxic effects on many species (Barker and Pilbeam, 2010).  
371 This observation is consistent with the recent assertion that *Betula* spp., and in particular, *B.*  
372 *pendula*, should be classified as hyperaccumulators of Zn, thereby having potential for Zn  
373 phytoremediation (Dmuchowski et al., 2014). Presumably, Pb evaded detection throughout  
374 the study because translocation from the roots is limited for many tree species, while  
375 restricted detection of Cu may be attributable to absorption that is often competitively  
376 inhibited by Zn (Kabata-Pendias and Pendias, 2001).

377

378 The observations for As and Zn described above are likely the result of differences in the  
379 accumulation, regulation, tolerance, translocation, exclusion and contribution of atmospheric  
380 deposition between the two elements and among the tree genera. Although determination of  
381 the precise causes for the contrasting behaviours of As and Zn would require further  
382 investigation, this study has clearly demonstrated the usefulness of FP-XRF in rapidly  
383 identifying such issues and its potential for guiding research iteratively and strategically.

384

### 385 **Conclusions**

386 This study has shown that FP-XRF configured in a low density mode is capable of  
387 determining certain trace elements, and in particular, As and Zn, on intact leaves from  
388 contaminated sites. With detection limits of a few tens of  $\mu\text{g g}^{-1}$  in both the fresh and dry  
389 states and good agreement with independent results from ICP analysis, the approach is  
390 suitable for the rapid throughput of samples with minimal preparation. As such, and when  
391 combined with a portable test stand, it also has the potential to be applied on site as a  
392 biomonitoring tool or for directly guiding a research plan strategically.

393

### 394 **Acknowledgements**

395 We are grateful to Drs Andrew Fisher and Alex Taylor, PU, for technical support throughout  
396 the study. This study was funded partly by a HEIF V Marine Institute grant.

397

### 398 **References**

399 Aničić, M., Spasić, T., Tomašević, M., Rajšić, S., Tasić, M., 2011. Trace elements  
400 accumulation and temporal trends in leaves of urban deciduous trees (*Aesculus*  
401 *hippocastanum* and *Tilia* spp.). Ecological Indicators 11, 824-830.

402



403 Antosiewicz, D.M., Escudé-Duran, C., Wierzbowska, E., Skłodowska, A., 2008. Indigenous  
404 plant species with the potential for the phytoremediation of arsenic and metals contaminated  
405 soil. *Water Air and Soil Pollution* 193, 197–210.

406

407 Baker, A.J.M., McGrath, S.P., Reeves, R.D., Smith, J.A.C., 2000. Metal hyperaccumulator  
408 plants: a review of the ecology and physiology of a biological resource for phytoremediation  
409 of metal polluted-soils. In: Terry, N., Bañuelos, G., Eds., *Phytoremediation*  
410 *of Contaminated Soil and Water*. Lewis Publishers, London, pp. 85-107.

411

412 Bargagli, R., 1998. *Trace Elements in Terrestrial Plants: An Ecophysiological Approach to*  
413 *Biomonitoring and Biorecovery*. Springer-Verlag, Berlin.

414

415 Bargagli, R., Monaci, F., Agnorelli, C., 2003. Oak leaves as accumulators of airborne  
416 elements in an area with geochemical and geothermal anomalies. *Environmental Pollution*  
417 124, 321-329.

418

419 Barker, A.V., Pilbeam, D.J. (Eds.), 2010. *Handbook of Plant Nutrition*. Taylor and Francis,  
420 Boca Raton, FL.

421

422 Bull, A., Brown, M.T., Turner, A., 2017. Novel use of field-portable-XRF for the direct  
423 analysis of trace elements in marine macroalgae. *Environmental Pollution* 220, 228-233.

424

425 Dimitrijević, M.D., Nujkić, M.M., Alagić, S.C., Milić, S.M., Tošić, S.B., 2016. Heavy metal  
426 contamination of topsoil and parts of peach-tree growing at different distances from a  
427 smelting complex. *International Journal of Environmental Science and Technology* 13, 615-  
428 630.

429

430 Dmuchowski, W., Gozdowski, D., Bragoszewska, P., Baczewska, A.H., Suwara, I., 2014.

431 Phytoremediation of zinc contaminated soils using silver birch (*Betula pendula* Roth).

432 Ecological Engineering 71, 32-35.

433

434 Environmental Protection Agency, 2007. Method 6200 - Field portable x-ray fluorescence

435 spectrometry for the determination of elemental concentrations in soil and sediment.

436 <http://www3.epa.gov/epawaste/hazard/testmethods/sw846/pdfs/6200.pdf>. Accessed 7/16.

437

438 Franiel, I., Babczyńska, A., 2011. The growth and reproductive effort of *Betula*

439 *pendula* Roth in a heavy-metals polluted area. Polish Journal of Environmental Studies 20,

440 1097-1101.

441

442 Hubbell, J.H., Seltzer, S.M., 1996. X-ray mass attenuation coefficients. National Institute of

443 Standards and Technology, Gaithersburg, Maryland.

444

445 Kabata-Pendias, A., Pendias, H., 2001. Trace Elements in Soils and Plants, third ed. CRC

446 Press, Boca Raton, Florida, USA.

447

448 Kalnicky, D.J., Singhvi, R., 2001. Field portable XRF analysis of environmental samples.

449 Journal of Hazardous Materials 83, 93-122.

450

451 Madejón, P., Marañón, Murillo, J.M., Robinson, B., 2004. White poplar (*Populus alba*) as a

452 biomonitor of trace elements in contaminated riparian forests. Environmental Pollution 132,

453 145-155.

454

455 Nirola, R., Megharaj, M., Palanisami, T., Arjal, R., Venkateswarlu, K., Naidu, R., 2015.  
456 Evaluation of metal uptake factors of native trees colonizing an abandoned copper mine e a  
457 quest for phytostabilization. *Journal of Sustainable Mining* 14, 115-123.  
458  
459 Pająk, M., Halecki, W., Gaşioerk, M., 2017. Accumulative response of Scots pine (*Pinus*  
460 *sylvestris* L.) and silver birch (*Betula pendula* Roth) to heavy metals enhanced by Pb-Zn ore  
461 mining and processing plants: Explicitly spatial considerations of ordinary kriging based on  
462 a GIS approach. *Chemosphere* 168, 851-859.  
463  
464 Radu, T., Diamond, D., 2009. Comparison of soil pollution concentrations determined using  
465 AAS and portable XRF techniques. *Journal of Hazardous Materials* 171, 1168–1171.  
466  
467 Rawlins, B.G., O'Donnell, K., Ingham, M., 2003. Geochemical survey of the Tamar  
468 catchment (south-west England). *British Geological Survey Report CR/03/027*, 232pp.  
469  
470 Sacristán , D., Viscarra Rossel, R.A., Recatalá, L., 2016. Proximal sensing of Cu in soil and  
471 lettuce using portable X-ray fluorescence spectrometry. *Geoderma* 265, 6-11.  
472  
473 Schmidt, M., Boras, S., Tjoa, A., Watanabe, T., Jansen, S., 2016. Aluminium accumulation  
474 and intra-tree distribution patterns in three *Arbor aluminosa* (*Symplocos*) Species from  
475 Central Sulawesi. *PLOS ONE* <https://doi.org/10.1371/journal.pone.0149078>  
476  
477 Serbula, S.M., Radojevic, A.A., Kalinovic, J.V., Kalinovic, T.S., 2014. Indication of  
478 airborne pollution by birch and spruce in the vicinity of copper smelter. *Environmental*  
479 *Science nad Pollution Research* 21, 11510-11520.  
480

481 Stefanowicz, A.M., Stanek, M., Woch, M.W., 2016. High concentrations of heavy metals in  
482 beech forest understory plants growing on waste heaps left by Zn-Pb ore mining. *Journal of*  
483 *Geochemical Exploration* 169, 157-162.  
484

485 Towett, E.K., Shepherd, K.D. and Drake, B.L., 2016. Plant elemental composition and  
486 portable X-ray fluorescence (pXRF) spectroscopy: quantification under different  
487 analytical parameters. *X-ray Spectrometry* 45, 117-124.  
488

489 Turner, A., Poon, H., Taylor, A., Brown, M.T., 2017. In situ determination of trace elements  
490 in *Fucus* spp. by field-portable-XRF. *Science of the Total Environment* 593-594, 227-235.  
491

492 Unterbrunner, R., Puschenreiter, M., Sommer, P., Wieshammer, G., Tlustos, P., Zupan, M.,  
493 Wenzel, W.W., 2007. Heavy metal accumulation in trees growing on contaminated sites in  
494 central Europe. *Environmental Pollution* 148, 107-114.  
495

496 Table 1: A comparison of measured and certified elemental concentrations in plastic, leaves  
 497 and soils. Errors represent the 95% confidence interval, with weighting for inter-method  
 498 variance where appropriate (certified), or two standard deviations about the mean (measured  
 499  $n$  times); asterisks denote indicative values.

		certified, $\mu\text{g g}^{-1}$ dw	measured, $\mu\text{g g}^{-1}$ dw
polyethylene disc, PN 180-619 XRF; $n = 10$	As	51 $\pm$ 7.0	46 $\pm$ 4.4
	Pb	150 $\pm$ 12	145 $\pm$ 9.2
peach leaves, GBW 08501 ICP; $n = 3$	As	0.34 $\pm$ 0.06	0.44 $\pm$ 0.04
	Cu	10.4 $\pm$ 1.6	8.0 $\pm$ 0.42
	Pb	0.99 $\pm$ 0.08	0.96 $\pm$ 0.04
	Zn	22.8 $\pm$ 2.5	23.3 $\pm$ 7.4
soil, NIST 2709 XRF; $n = 5$	As	10.5 $\pm$ 0.3*	9.3 $\pm$ 2.3
	Cu	33.9 $\pm$ 0.5*	26.3 $\pm$ 6.1
	Pb	17.3 $\pm$ 0.1	12.9 $\pm$ 3.4
	Zn	103 $\pm$ 4.0*	97.5 $\pm$ 8.1
soil, MSH-100 XRF; $n = 5$	As	1090 $\pm$ 16.7	999 $\pm$ 24.0
	Zn	1100 $\pm$ 16.8	1047 $\pm$ 36.0

501

502 Table 2: Number and distribution of leaf samples used in the present study.

sampling site	<i>Fagus</i>	<i>Betula</i> spp.	<i>Quercus</i> spp.
S1	15	9	9
S2	3	3	12
S3	9	18	9
total	27	30	30

503

504

505 Table 3: A summary of the characteristics of the soil samples from the three sites, shown as  
 506 the mean and one standard deviation for each parameter.

sampling site	pH	As, $\mu\text{g g}^{-1}$ dw	Cu, $\mu\text{g g}^{-1}$ dw	Pb, $\mu\text{g g}^{-1}$ dw	Zn, $\mu\text{g g}^{-1}$ dw
S1 ( $n = 3$ )	5.53 $\pm$ 0.68	183 $\pm$ 60	356 $\pm$ 192	103 $\pm$ 34.1	192 $\pm$ 35.3
S2 ( $n = 3$ )	4.89 $\pm$ 0.83	9310 $\pm$ 8470	1070 $\pm$ 858	159 $\pm$ 73	125 $\pm$ 33.9
S3 ( $n = 3$ )	5.40 $\pm$ 0.74	24,200 $\pm$ 6620	1380 $\pm$ 453	254 $\pm$ 44.9	187 $\pm$ 89

507

508

509

510 Table 4: Mean and, in parentheses, minimum and maximum XRF measurement detection  
 511 limits for trace elements in fresh and freeze-dried leaf samples.

	As	Cu	Pb	Zn
fresh ( $n = 87$ ), $\mu\text{g g}^{-1}$ fw	12.9 (4.5-47.9)	71.3 (29.2-215)	26.7 (10.9-83.4)	33.5 (15.6-113)
512 dry ( $n = 87$ ), $\mu\text{g g}^{-1}$ dw	21.2 (9.9-52.9)	116 (59.1-353)	42.9 (19.2-118)	56.9 (22.6-189)

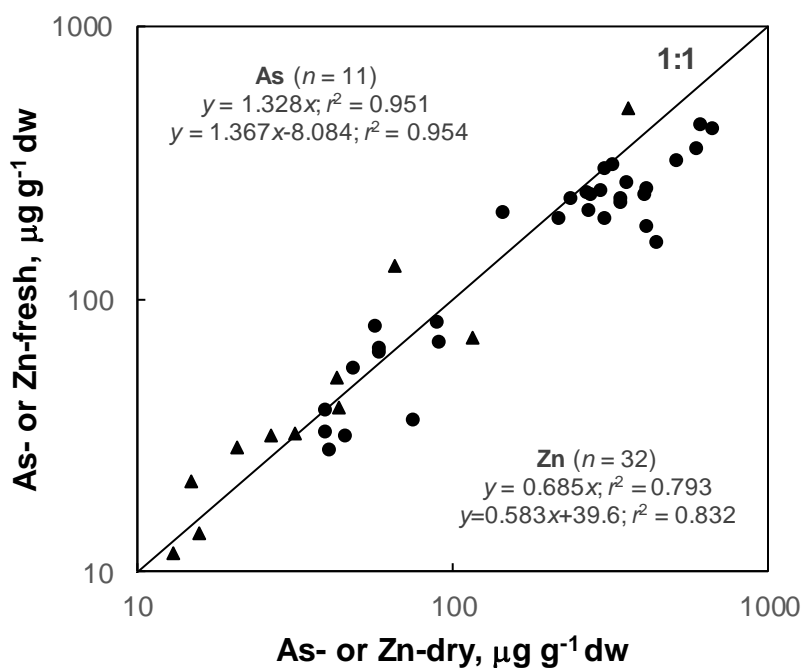
513

514 Table 5: The number of cases that each element was detected among the leaf samples  
 515 analysed ( $n$ ) and summary statistics for the resulting concentrations.

		As	Cu	Pb	Zn
XRF-fresh, $\mu\text{g g}^{-1}$ fw	$n$	19	0	0	40
	mean	47.5			92.4
	median	20.3			89.3
	min	5.2			21.0
	max	450			280
XRF-fresh, $\mu\text{g g}^{-1}$ dw	$n$	19	0	0	40
	mean	60.0			169
	median	28.4			192
	min	11.7			28.0
	max	501			436
XRF-dry, $\mu\text{g g}^{-1}$ dw	$n$	13	2	0	47
	mean	63.5	71.3		208
	median	37.6	71.3		175
	min	12.9	62.0		27.6
	max	361	80.6		661
ICP, $\mu\text{g g}^{-1}$ dw	$n$	28	28	28	28
	mean	28.0	12.9	4.4	76.6
	median	1.4	8.7	2.4	23.1
	min	0.04	3.7	0.52	2.7
	516 max	503	85.6	25.6	344

517

518



520

521

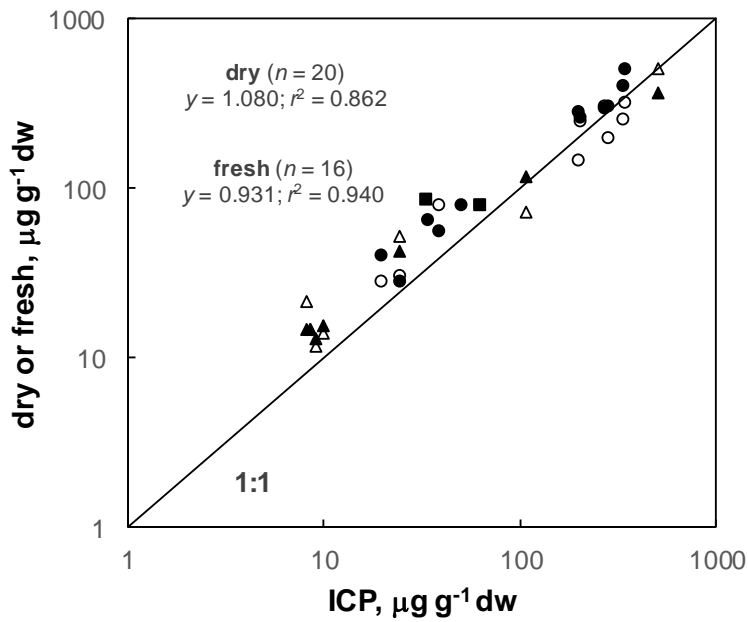
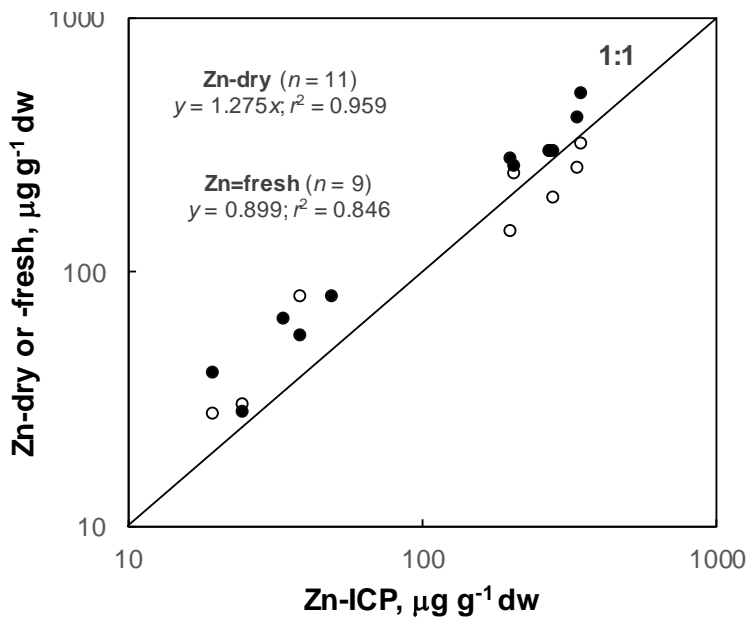
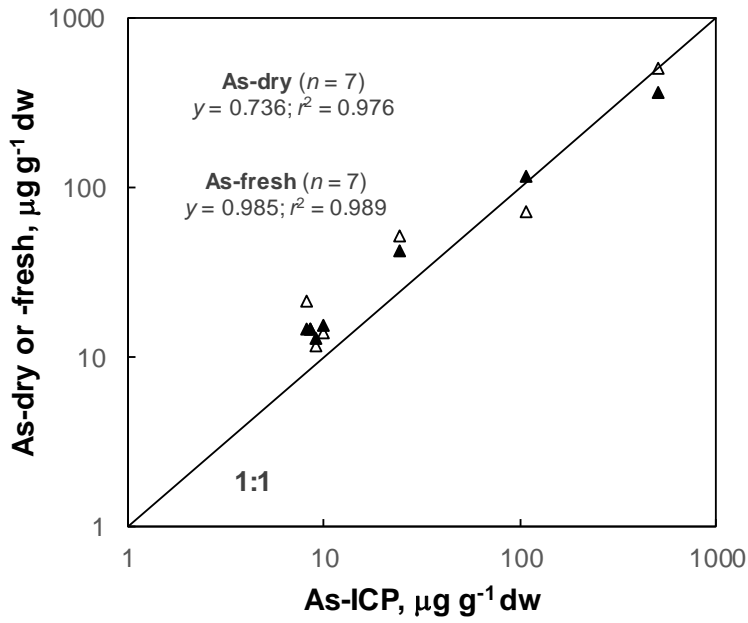
522 Figure 1: A comparison of dry weight leaf concentrations of As ( $\blacktriangle$ ) and Zn ( $\bullet$ ) derived from  
 523 fresh analysis by XRF and correction for water content and returned by direct analysis by  
 524 XRF. The solid line denotes unit slope and regression equations and coefficients of  
 525 determination defining the data sets are annotated.

526

527



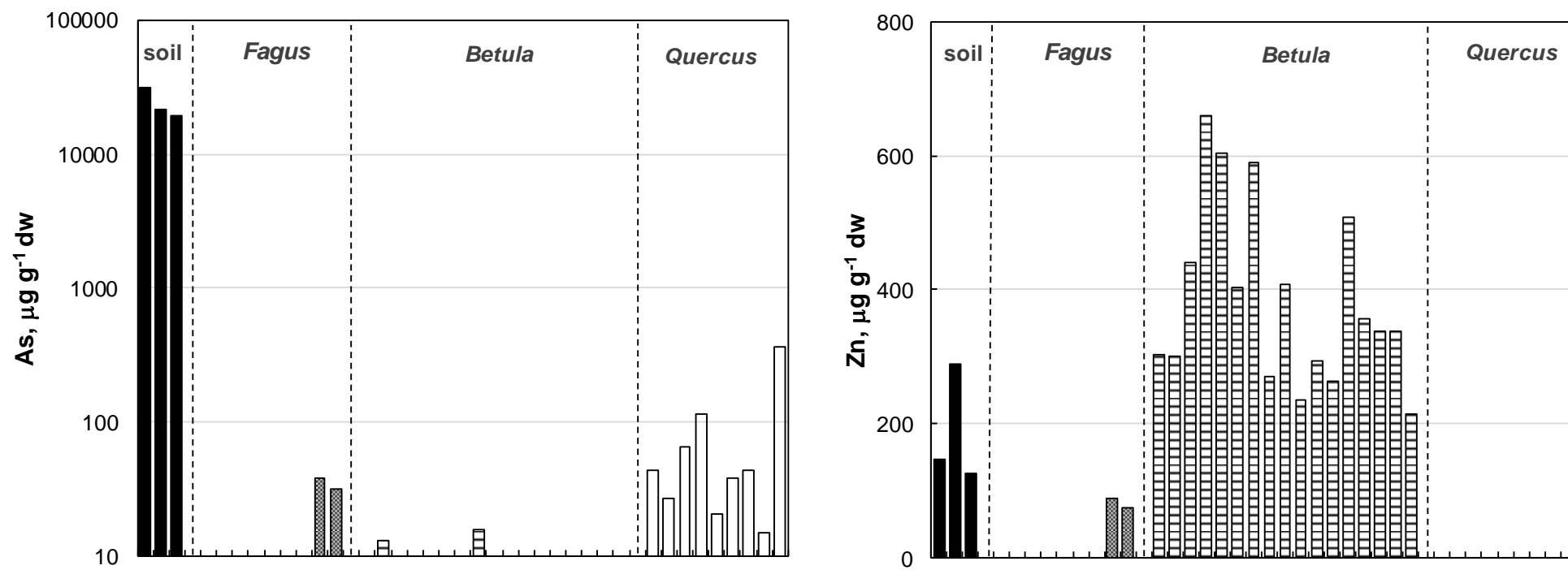




530

531 Figure 2: A comparison of the dry weight concentrations of trace elements in leaves  
532 determined by ICP following acid digestion and by XRF (As analysed fresh,  $\Delta$ , and dry,  $\blacktriangle$ ;  
533 Zn analysed fresh,  $\circ$ , and dry,  $\bullet$ ; Cu analysed dry,  $\blacksquare$ ). The solid line denotes unit slope and  
534 regression equations and coefficients of determination defining the data sets are annotated.

535 Figure 3: Concentrations of As and Zn, where detected, in the individual soil and tree leaf samples from S3.



536

537

538